

Provided for non-commercial research and education use.
Not for reproduction, distribution or commercial use.



This article appeared in a journal published by Elsevier. The attached copy is furnished to the author for internal non-commercial research and education use, including for instruction at the authors institution and sharing with colleagues.

Other uses, including reproduction and distribution, or selling or licensing copies, or posting to personal, institutional or third party websites are prohibited.

In most cases authors are permitted to post their version of the article (e.g. in Word or Tex form) to their personal website or institutional repository. Authors requiring further information regarding Elsevier's archiving and manuscript policies are encouraged to visit:

<http://www.elsevier.com/authorsrights>



Contents lists available at ScienceDirect

European Polymer Journal

journal homepage: www.elsevier.com/locate/europolj

Free-radical polymerization induced macrophase separation in poly(methyl methacrylate)/dimethacrylate blends: Experiment and modeling



Walter F. Schroeder*, Mirta I. Aranguren, Guillermo E. Eliçabe, Julio Borrajo

Institute of Materials Science and Technology (INTEMA), University of Mar del Plata – National Research Council (CONICET), Av. Juan B. Justo 4302, 7600 Mar del Plata, Argentina

ARTICLE INFO

Article history:

Received 26 April 2013

Received in revised form 23 July 2013

Accepted 30 August 2013

Available online 13 September 2013

Keywords:

Polymerization-induced phase separation

Thermoplastic-thermoset blends

Dimethacrylate

Phase behavior

Crosslinked polymer

ABSTRACT

This work presents the analysis of a polymerization-induced macrophase separation taking place during free-radical copolymerization of styrene and dimethacrylate in the presence of poly(methyl methacrylate) (PMMA) as a modifier. The PMMA does not participate in the polymerization but induces phase separation in the course of the reaction. An experimental study based on real-time static light scattering measurements with the aim of monitoring the phase behavior during the isothermal copolymerization is firstly presented. Then, an original and innovative contribution is made by modeling the evolution of the unstable region of the phase diagram as a function of conversion and by predicting phase separation in spinodal condition. The analysis is performed using an expression for the free energy of a reactive network-forming mixture based on the Flory–Rehner lattice model for swollen gels. The accuracy of the proposed model is verified by the good agreement found between its predictions and the experimental results.

© 2013 Elsevier Ltd. All rights reserved.

1. Introduction

Polymerization-induced phase separation (PIPS) finds application in the synthesis of a set of useful materials such as high-impact polystyrene (HIPS) [1], thermoplastic-thermoset blends [2], polymer-dispersed liquid crystals [3], thermally reversible light scattering films [4], nanoporous polymer materials [5,6], nanostructured thermosets [7], and macroporous materials [8] which have been extensively applied for separation (beads, membranes, monoliths), analysis (various kinds of chromatography) and in many branches of technology including medicine [9] (tissue engineering, drug delivery).

The PIPS method consists of polymerizing the precursor monomers in the presence of an additional component (e.g. modifier), such as an oligomer, a polymer, or a small

molecule. During polymerization, a phase separation process takes place leading to different types of morphologies that depend on the initial composition and reaction conditions [10–13]. The ultimate properties of these materials depend on the morphologies generated in the course of the reaction [14]. Linear polystyrene was one of the first additives used to cause phase separation and to give place to macroporous materials based in styrene–divinylbenzene resins. In this case, it was shown that phase instability was very sensitive to the molecular weight of polystyrene [15]. Thus, understanding the thermodynamic principles that lead to phase separation becomes very useful in designing new materials. In addition, the ability of predicting phase behavior can help to avoid the trial-and-error procedures that are used in most cases. In this report, we present a thermodynamic model that allows to simulate the phase-separation process induced by free-radical polymerization of styrene (St) and bisphenol A glycidyl methacrylate (BisGMA) in the presence of poly(methyl methacrylate) (PMMA) as a modifier.

* Corresponding author. Tel.: +54 (223) 481 66 00; fax: +54 (223) 481 00 46.

E-mail address: wshroeder@fi.mdp.edu.ar (W.F. Schroeder).

A thermodynamic description of PIPS shows that the main driving force for phase separation is the decrease of the absolute value of the entropic contribution to the Gibbs free energy of mixing [16]. Other factors can also contribute to the demixing process such as a change in the interaction parameter due to changes in the chemical structure produced by polymerization or the development of elastic energy after gelation (in the case of a thermosetting polymer) [17]. Models that allow a good description of the PIPS process in systems that polymerize by a stepwise mechanism have been recently reported [18–20]. For this type of polymerization, statistical models that successfully describe the evolution of the species distributions as a function of conversion have been developed. If the presence of the modifier does not significantly affect such distributions, it is possible to combine the polymerization statistic model with a thermodynamic model, such as the lattice theory of Flory–Huggins [21], to successfully describe the PIPS process.

For chainwise polymerizations, the simplest case is illustrated by the polymerization of a vinyl monomer (styrene, (meth)acrylic monomer, etc.) in the presence of a modifier, leading to a linear polymer. Several recent papers have analyzed PIPS in this type of systems [12,22–24]. However, for thermosetting systems polymerizing by a chainwise mechanism the situation is much more complex. In these cases, the development of a polymerization statistic model is very difficult, due to the formation of highly crosslinked domains containing numerous intramolecular rings that do not contribute to the elastic properties of the network. Thus, in the few models that have been proposed, it has been necessary to introduce strong hypothesis on these aspects, and so predictions are of qualitative nature [25,26].

Our aim is to provide a thermodynamic description of PIPS in a reactive network-forming system polymerizing by a chainwise mechanism. The selected system is a dimethacrylate(BisGMA)/St resin containing PMMA as a thermoplastic modifier. The PMMA does not participate in the co-polymerization but induces phase separation in the course of the reaction. In general terms, the phase diagram of the St–BisGMA–PMMA ternary blend represents the initial thermodynamic state of the reactive system at zero conversion. This phase diagram has been studied and discussed in previous works [11,27]. Here, we are concerned with the phase behavior during reaction, when the system consists of four components, St, BisGMA, copolymer (St-co-BisGMA), and PMMA. The phase state of such a system should be represented by means of a quaternary phase diagram that describes the phase evolution by effect of conversion, an issue that to our knowledge has not been previously analyzed in the literature.

Phase separation can occur either by the nucleation and growth (NG) mechanism in the metastable region of the phase diagram, or by spinodal decomposition (SD) if the system becomes unstable. Depending on the relative rates of phase separation and polymerization, the compositional trajectory may be fully located in the metastable region, in which case phase separation would take place exclusively by an NG mechanism, or it may enter the unstable region, implying that SD has to be considered to account for the

morphology generated. Since the homogeneous nucleation is a slow process in comparison to SD [28], frequently the mixture quickly passes through the metastable region and then enters the unstable region where the spinodal decomposition process is initiated by small concentration fluctuations throughout the sample [29]. In the early stages of SD the amplitude of the concentration fluctuations increases while the characteristic distance between fluctuations remains constant. This event gives place to the appearance of a correlation peak located at a nonzero constant scattering vector (q), when the phase separation process is followed by light scattering experiments [30,31].

In this article we first present an experimental study based on real-time static light scattering measurements with the aim of monitoring the phase behavior during the isothermal copolymerization of St and BisGMA in the presence or not of a thermoplastic modifier. Then, a thermodynamic model of PIPS is introduced and its predictions are compared with the experimental results. In our thermodynamic analysis, we apply an expression for the free energy of a reactive network-forming mixture based on the Flory–Rehner lattice model for swollen gels [32] later modified by Dušek et al. [33]. This expression allows us to compute the evolution of the unstable region limited by the spinodal curve as a function of conversion. In this approach, it is assumed that the speed at which the trajectory crosses the metastable region on the phase diagram is sufficiently fast, such that no nuclei can be created during this time interval. Consequently, the isothermal phase separation process is strictly spinodal decomposition. We will present experimental evidence that supports such an assumption.

2. Theoretical background

Phase separation in reactive network-forming systems can be analyzed using the Flory–Rehner lattice model for swollen gels [32], later modified by Dušek et al. [33]. For a mixture of i components, the dimensionless mixing Gibbs free energy per mole of lattice sites is expressed as

$$\frac{\Delta G^{mix}}{MRT} = \sum_i \frac{\phi_i}{x_i} \ln \phi_i + \sum_{ij} \chi_{ij} \phi_i \phi_j + v_e \varepsilon \phi_g \left[\frac{3}{2} \left(\phi_g^{-\frac{2}{3}} - 1 \right) + \frac{2}{f} \ln \phi_g \right] \quad (1)$$

where R is the gas constant, T is the absolute temperature, and M is given by $M = \sum_i n_i x_i$ and represents the number of moles of cells in the system; n_i is the number of moles of the i -component, and x_i the number of cells occupied by i -component. The cell volume was taken as 116.85 cm³/mol, which corresponds to the molar volume of St monomer. ϕ_i and ϕ_j are the volume fractions of components i and j respectively.

The first two terms on the right side of Eq. (1) represent the entropic and enthalpic contributions to the free energy expressed in terms of the binary interaction parameters, χ_{ij} ($\chi = a + b/T$, where a and b are constants); while the last term represents the elastic contribution to the free energy, which appears in the postgel stage of the reaction. ϕ_g is the

volume fraction of gel, v_e represents the number of chains between crosslinking points per mole of cells occupied by the gel, and ε is the fraction of these chains that have elastic behavior. This last parameter is introduced because cycles are formed during polymerization, and the chains forming these cycles do not contribute to the elastic properties of the network. Thus, $v_e \varepsilon \phi_g$ is the number of moles of elastic active chains per mole of cells.

As reported by Dušek for divinyl–monovinyl monomer copolymerization forming networks [34], ε can take values between 0.3 and 0.9, depending on the divinyl monomer concentration and the rigidity of the polymer chain that forms the network. In this study, an arbitrary value within that range, $\varepsilon = 0.50$, was considered. Regarding the number of chains between crosslinking points, we assumed that all divinyl monomers with both double bonds reacted act like crosslinking points in the gel, the same consideration made by Dušek [33] and Boots et al. [35]. Taking into account that each double bond of divinyl monomers has a crosslinking functionality $f = 3$, the parameter v_e is expressed by the following equation:

$$v_e = \frac{3}{2} \alpha_1^2 f_{1,0} \quad (2)$$

where α_1^2 represents the probability that a reacted BisGMA extreme belongs to a double-reacted BisGMA molecule. $f_{1,0}$ is the initial molar fraction of BisGMA double bonds, and the 3/2 factor represents the number of chains leaving a crosslinking point.

The mixing Gibbs free energy written explicitly in terms of the four components of the system is then,

$$[G]_{P,T,\alpha} = \frac{\Delta G^{mix}}{MRT} = \left(\frac{\phi_0}{x_0} \ln \phi_0 + \frac{\phi_1}{x_1} \ln \phi_1 + \frac{\phi_2}{x_2} \ln \phi_2 + \frac{\phi_3}{x_3} \ln \phi_3 + \chi_{01} \phi_0 \phi_1 + \chi_{02} \phi_0 \phi_2 + \chi_{03} \phi_0 \phi_3 + \chi_{12} \phi_1 \phi_2 + \chi_{13} \phi_1 \phi_3 + \chi_{23} \phi_2 \phi_3 + v_e \varepsilon \phi_g \left[\frac{3}{2} (\phi_g^{-\frac{1}{2}} - 1) + \frac{2}{3} \ln \phi_g \right] \right) \quad (3)$$

where the subscripts represent: St(0), BisGMA(1), copolymer(2), and PMMA(3). Note that the last term of the summation (e.g. the elastic term) only contributes in the postgel stage of the reaction. To simplify the analysis, the entire polymer will be considered to form part of the gel phase once reached the gel point, consequently $\phi_g = \phi_2$ and the term $\frac{\phi_2}{x_2} \ln \phi_2$ becomes zero at the postgel stage of the reaction.

At any level of double bond conversion in the liquid–liquid or liquid–gel phase diagram, three regions can be defined: stable, metastable, and unstable (spinodal). These regions are differentiated by stability criteria for a homogeneous phase [21]. In this work, we analyze phase separation in the reactive St–BisGMA–copolymer–PMMA quaternary system by computing the evolution of the unstable region, limited by the spinodal decomposition curve, as a function of conversion.

The spinodal condition is given by [21]

$$Y = \left| \frac{\partial^2 \Delta G^{mix}}{\partial \phi_i \partial \phi_j} \right|_{P,T,\alpha} = 0 \quad (4)$$

where Y represents the determinant of mixing Gibbs free energy second derivatives with respect to the independent compositions of the system. A homogeneous phase is

unstable if $Y < 0$. In the region where $Y > 0$, a homogeneous phase may exist in stable or metastable conditions.

2.1. Calculation method

To compute the evolution of the spinodal decomposition curve as a function of conversion, it is necessary to relate concentrations of St, BisGMA, and copolymer (as well as its composition and molar mass) with the global conversion of reaction. It was considered that an initial number of moles of double bonds, N_0 , reacted in N_0 steps (1 mol per step). Ignoring the effects of PMMA modifier, the molar fraction of St in the copolymer for a step $i + 1$, $F_{0,i+1}$, can be calculated from a general balance:

$$F_{0,i+1} = \frac{r_{0,i} f_{0,i}^2 + f'_{0,i} f'_{1,i}}{r_{0,i} f_{0,i}^2 + 2f'_{0,i} f'_{1,i} + r_{1,i} f_{1,i}^2} \quad F_{1,i+1} = 1 - F_{0,i+1} \quad (5)$$

where the subscripts 0 and 1 represent St and BisGMA, respectively. $F_{1,i+1}$ is the molar fraction of double bonds of BisGMA added to the copolymer in the step $i + 1$; and f' represents the molar fraction of double bonds in the feed.

$$f'_{0,i+1} = \frac{(N_0 - i) f'_{0,i} - F_{0,i+1}}{N_0 - (i + 1)} \quad f'_{1,i+1} = 1 - f'_{0,i+1} \quad (6)$$

$r_{0,i}$ and $r_{1,i}$ are the reactivity ratios of St and BisGMA in the step i , which were evaluated from the following equations [36]

$$r_{0,i} = r_{0,0} (1 - (\alpha_i / \alpha_u))^R \quad r_{1,i} = r_{1,0} (1 - (\alpha_i / \alpha_u))^S \quad (7)$$

where $r_{0,0}$ and $r_{1,0}$ are the reactivity ratios of St and BisGMA at zero conversion and their values were previously determined as 0.43 ± 0.03 and 0.41 ± 0.05 , respectively [36]; α_i is the global conversion in the step i ; α_u is the global conversion at the end of the reaction; and R ($= -0.61$) and S ($= 1.06$) are empirical fitting parameters also evaluated in a previous study [36].

From Eqs. (5)–(7), F and f can be computed for each reaction step. Double bond conversions of both reactants and global conversion can then be calculated:

$$\alpha_{0,i+1} = \alpha_{0,i} + \frac{F_{0,i+1}}{N_0 f'_{0,0}} \quad \alpha_{1,i+1} = \alpha_{1,i} + \frac{F_{1,i+1}}{N_0 f'_{1,0}} \quad (8)$$

$$\alpha_{i+1} = \frac{\alpha_{0,i+1} f'_{0,0} + \alpha_{1,i+1} f'_{1,0}}{f'_{0,0} + f'_{1,0}}$$

Once evaluated the conversions, the volume fraction of each component in the step $i + 1$ of the reaction can be computed. Considering that the total volume does not change upon reaction (see Supporting Information), the volume fraction of each monomer in the copolymer is:

$$\phi_{0,i+1}^c = \frac{\alpha_{0,i+1} \frac{f_{0,0} M_0}{\rho_0}}{\alpha_{0,i+1} \frac{f_{0,0} M_0}{\rho_0} + (\alpha_{1,i+1}^2 + 2\alpha_{0,i+1} \alpha_{1,i+1}) \frac{f_{1,0} M_1}{\rho_1}} \quad (9)$$

$$\phi_{1,i+1}^c = 1 - \phi_{0,i+1}^c$$

where M_0 and M_1 represent the molar mass of St and BisGMA respectively, and ρ_0 and ρ_1 the corresponding densities.

To compute the spinodal decomposition curve at a particular conversion, it is necessary to know the interaction parameters between the copolymer and the other species, which can be calculated from the segmental interaction parameters [37]. In a mixture of a homopolymer A and a random copolymer $B_xC_{(1-x)}$, the interaction parameter between homopolymer and copolymer can be written as:

$$\chi_{A,\text{copol}} = \phi_B^c \chi_{AB} + (1 - \phi_B^c) \chi_{AC} - \phi_B^c (1 - \phi_B^c) \chi_{BC} \quad (10)$$

In our case, the following segmental interaction parameters are needed:

$$\chi_{\text{St-HBisGMA}} = \chi_{\text{HSt-BisGMA}} = \chi_{01}$$

$$\chi_{\text{HSt-PMMA}} = \chi_{03} \quad (11)$$

$$\chi_{\text{HBisGMA-PMMA}} = \chi_{13}$$

where HSt and HBisGMA represent the segments of St and BisGMA in the copolymer and are assumed to be equivalent to the monomers. The subscript 3 represents the PMMA modifier. The third term on the right side of Eq. (10) requires the knowledge of the interaction parameter HSt-HBisGMA (χ_{H0H1}), which is an empirical parameter assumed to be 3.3×10^{-2} . It should be highlighted that χ_{H0H1} is the only fitting χ -parameter required for modeling the quaternary blends and it is valid in the whole range of the analyzed compositions. The remainder of χ -parameters is obtained from the analysis of the individual binary systems.

Thus, the resulting equations are:

$$\chi_{02,i} = \phi_{1,i}^c \chi_{01} - \phi_{0,i}^c \phi_{1,i}^c \chi_{\text{H0H1}}$$

$$\chi_{12,i} = \phi_{0,i}^c \chi_{01} - \phi_{0,i}^c \phi_{1,i}^c \chi_{\text{H0H1}} \quad (12)$$

$$\chi_{23,i} = \phi_{0,i}^c \chi_{03} + \phi_{1,i}^c \chi_{13} - \phi_{0,i}^c \phi_{1,i}^c \chi_{\text{H0H1}}$$

Finally, to represent the evolution of the relative size of the copolymer as a function of conversion in the pregel stage of the reaction, the approach proposed by Okay et al. for free-radical cross-linking copolymerization of vinyl/divinyl monomers, was used [38]. The expression can be written as

$$x_{2,i} = x_{2,0} (1 - (\alpha_i / \alpha_g))^{-\gamma} \quad (13)$$

where γ is the critical exponent and its value is 1.6 ± 0.2 [38]; α_g is the gel point conversion taken equal to 0.08 [39]; and $x_{2,0}$ is the relative size of the copolymer at the start of the reaction and its assumed value is 600 [38]. It is stressed that all these values are not fitting parameters, and that they are taken from results obtained from similar polymer systems, which have been already published [38,39]. With the previous equations, the spinodal decomposition curve can be calculated for the global conversion corresponding to each reaction step.

It is worth pointing out that the present model only takes into account the elastic contribution to the free energy once the macrogelation was reached (Eq. (2)). However, one characteristic of the network formation process in free radical polymerization is the spatial heterogeneity in the reacting system. The formation of microgels in the

early stages of the polymerization is the primary cause of structural heterogeneity in the network. Microgels are densely cross-linked and cyclized polymers and result from the formation of highly cross-linked regions near the site of the initiated radical. These microgels should have some elastic contribution to the free energy at early stages of polymerization prior to the macrogelation. Such a contribution is very difficult of evaluating and is not taken into account in the present analysis.

3. Experimental

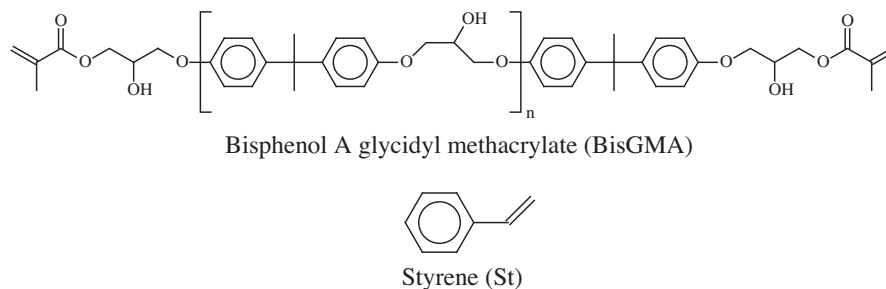
3.1. Materials and sample preparation

Bisphenol A glycidyl methacrylate (BisGMA) (Esstech, Essington, PA), styrene (St) (Poliresinas San Luis S.A., San Luis, Argentina), and poly(methyl methacrylate) (PMMA) (Aldrich Chemical Company) were used as received. The structures of both co-monomers (BisGMA and St) are shown in Scheme 1. The molar mass averages of BisGMA were determined by size exclusion chromatography (SEC) (Waters Model 440, Waters, Milford, MA) using columns PLGel (Torrance, CA) of 100, 500, 10^3 , 10^4 , and 10^6 Å in distilled tetrahydrofuran with polystyrene calibration. The molar mass distribution of PMMA was also measured by SEC (Waters ALC 244, Milford, MA) at 25 °C using Shodex columns (Milford, MA) A 802, 803, 804, 805, and 806/S with both refraction index and specific viscosity detection on line (Viscotek Model 200, Houston, TX) using universal calibration curve determined with polystyrene standards and the Mark-Houwink constants of PMMA in THF at 25 °C [40]: $a = 0.697$; $K = 10.4 \times 10^{-3}$ mL/g. Molar mass averages and other characteristics of the components used in this study are reported in Table 1.

Solutions of St/BisGMA = 45/55 wt% containing PMMA in a proportion of 5 and 20 wt% were prepared. The PMMA particles were initially dissolved in part of the St, and then they were mixed with the BisGMA and the remaining St to reach the final composition. All the samples were cured at 80 °C using benzoyl peroxide 2 wt% (Luzidol 75%, Akzo Chemicals S.A., Buenos Aires, Argentina) as the initiator of the free radical polymerization.

3.2. Infrared spectroscopy

FTIR curing studies were performed using a Genesis II Mattson FTIR (Mattson, Madison, WI) spectrometer in the transmission mode. A drop of the sample containing initiator was sandwiched between two KBr crystal discs separated by a 50 µm aluminum spacer ring used to regulate the sample thickness and to avoid evaporation of styrene. The assembly was placed in a sample oven HT-32 (Spectra-Tech Inc., Shelton, CT) with programmable temperature control, which was then mounted into the spectrometer. A thermocouple (K-type) was directly plunged into the reactive mixture to record the real temperature of the system during reaction. The temperature was kept within 80 ± 0.5 °C and FTIR measurements were taken in real time. FTIR spectra were acquired in absorbance mode over the range of 600–2000 cm^{-1} from 8 coadded scans at



Scheme 1. Chemical structures of the co-monomers.

Table 1

Characterization of the used components.

	St (0)	BisGMA (1)	PMMA (3)
M_n (g/mol)	104	600 ^a	41500 ^a
M_w/M_n	1.00	1.06	1.93
Density _{25 °C} (g/cm ³)	0.91 ^b	1.16 ^b	1.19 ^c

^a Measured by SEC, THF solvent at 1 mL/min.^b Measured using a precision balance for densities.^c Taken from the supplier's catalog.

2 cm⁻¹ resolution. The sampling interval was 3 min until no changes were observed in the absorbance peak area. The conversion profiles were calculated from the decay of the absorption bands located at 945 cm⁻¹ (C=C in BisGMA) and 910 cm⁻¹ (C=C in St) as described in the literature [41]. The overall conversion of C=C double bonds (α) was determined as

$$\alpha(t) = f_{0,0}\alpha_0(t) + f_{1,0}\alpha_1(t) \quad (14)$$

where $f_{i,0}$ is the initial molar fraction of double bonds of St ($i = 0$) or BisGMA ($i = 1$), and $\alpha_i(t)$ is the fractional conversion of double bonds of each one at time t .

3.3. Light Scattering (LS)

Static light scattering experiments were performed using a Fraunhofer configuration LS apparatus consisting of a linear array of 224 photodiodes placed to detect the scattered light at different angles by a thin sample illuminated by a 17 mW He–Ne laser with random polarization. The sample was sandwiched between two glass windows separated by a 1.2 mm spacer ring. This assembly was placed into an aluminum block provided with a computer-controlled electrical heating system. A K-type thermocouple directly plunged into the sample was used to monitor the real temperature of the system, which was kept within 80 ± 1 °C. The intensity of scattered light from the sample was collected by 14 common cathode monolithic silicon photodiode linear arrays of 16 elements each, manufactured by Photonics Detectors Inc. An opal diffusing glass was used to calibrate the photodiodes individually and thus compensate for their different gains. The current flow from the photodiode circulated through a resistance generating a voltage proportional to the incident light. Signals were sent to a microprocessor that carried out all the coordination and control tasks, connected to a personal computer through a serial port. This type of connection im-

posed a minimum sampling time of 1 s, although the time needed to collect a whole spectrum was considerably smaller.

The same formulations selected to evidence phase separation by LS were also used to follow its double-bond conversion by FTIR. A thermocouple plunged into the sample in both LS and FTIR setups allowed us verifying that the real temperature of the sample in both experiments was virtually the same during the whole reaction. The phase separation time was evidenced by the beginning of an increase in the intensity of the scattered light. The knowledge of the kinetics of double bond conversion enabled us to transform the time scale into a conversion scale.

4. Results and discussion

4.1. Phase separation during polymerization

Phase separation in the course of polymerization of St/BisGMA (45/55 wt%) solutions containing 0, 5 and 20 wt% PMMA as a modifier was investigated by real-time static light scattering (LS). At the same time, real-time FTIR studies under the same reaction conditions were carried out in order to transform the time data of the light scattering experiments into double bond conversion data. All the reactions were studied in isothermal conditions at 80 °C.

Fig. 1 shows the light scattering intensity at four q vector values (2.81, 3.32, 4.16, and 4.97 μm^{-1}) together with

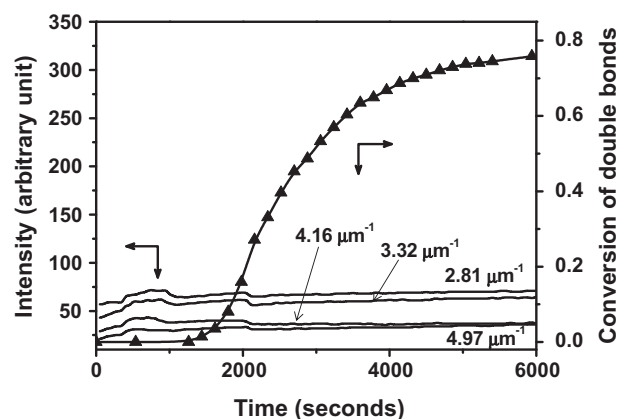


Fig. 1. Overall conversion of double bonds and light scattering intensity at different values of q vector plotted as a function of reaction time for the St/BisGMA mixture with no PMMA added cured at 80 °C. Line connecting conversion points is drawn to guide the eye.

the overall double bond conversion plotted as a function of time for the whole reaction of the St/BisGMA mixture without PMMA added. It can be seen that while conversion increases to get a value equal to 0.77 at 6000 s of reaction, the light scattering intensity at the different angles remains low and virtually constant indicating little change in the morphology of the sample during the course of reaction. This result suggests that no phase separation takes place during polymerization of the St/BisGMA sample without PMMA added. In a previous paper [42] we showed that the St–BisGMA thermoset without PMMA added was a transparent, homogeneous material with a flat fracture surface that showed no phase-separation features by SEM, confirming our previous interpretation of the LS data that no polymerization induced phase separation takes place in the sample without added PMMA.

Samples containing PMMA presented a different behavior. Fig. 2 shows the profiles of light scattering intensity at four q values and the double bond conversion curve as a function of time for the sample containing 5 wt% PMMA. Three different regions in the LS profiles can be distinguished. The first one agrees with the induction period of the reaction. Here, no changes in the morphology of the sample occur as the polymerization reaction has not still started. Consequently, the light scattering intensity remains practically constant indicating that the system is still homogeneous. A second region characterized by a pronounced increase in the LS intensity starts at very early stages of the polymerization reaction, as observed on the conversion curve. This increase in the LS intensity indicates pronounced changes in the morphology of the sample associated to the beginning of the phase separation. The double bond conversion for the onset of phase separation is $\alpha = 0.02$. As phase separation progresses, the LS intensity increases indicating that the concentration of BisGMA, St and PMMA are continuously evolving in the separating phases. The LS intensity grows up to reach a maximum value at double bond conversion close to $\alpha = 0.07$. This value is very close to the gelation conversion for this system, which is between 0.08 and 0.10 as it has been reported in a previous study [39]. This suggests that the evolution

of the phase separation in this system would be strongly hindered by gelation. In the third region, which covers the remainder of the test, the LS intensity slowly decreases as the crosslinking reaction progresses. The decrease of the scattering peak in systems undergoing a polymerization induced phase separation has also been observed by other authors and attributed to the matching of refractive indices of both phases [43]. As the crosslinking reaction advances, the refractive index difference (e.g. contrast) between the PMMA and the crosslinked St–BisGMA resin become lower compared to the contrast between St/BisGMA and PMMA before reaction. Regarding the St–BisGMA crosslinking reaction, it can be seen in Fig. 2 that the conversion curve progresses almost exclusively in the third region of the LS profiles, indicating that the co-polymerization reaction mostly occurs in a phase separated system with a structure fixed by gelation.

Fig. 3 shows the results obtained for the sample with 20 wt% PMMA. Qualitatively, the LS profiles present the same trends observed for the sample with 5 wt% PMMA. However, it is clear that the growth in the LS intensity, associated to the phase separation process (second region), is much faster than that obtained with 5 wt% PMMA. This result is a consequence of the higher concentration of PMMA in this sample. Due to this, a larger amount of PMMA is segregated in the same period of time from the mother phase producing a faster increase of the relative intensity of light scattered at the different scattering angles. It can also be seen in Fig. 3 that the LS profiles get a maximum at a lower conversion value than for 5 wt% PMMA (Fig. 2), suggesting that the phase separation is hindered by viscosity in the pregel stage of the reaction. This idea is consistent with the fact that the initial viscosity of the sample with 20 wt% PMMA is much higher than that with 5 wt% PMMA.

Fig. 4 shows the light scattering spectra recorded at selected increasing times for the sample with 20% PMMA. One can see the presence of a scattering maximum at a q value that remains constant during the experiment. The LS spectra corresponding to the sample with 5 wt% PMMA presented similar features. The existence of a scattering

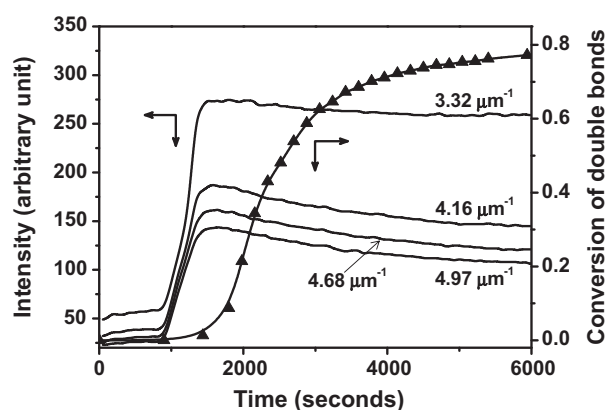


Fig. 2. Overall conversion of double bonds and light scattering intensity at different values of q vector plotted as a function of reaction time for the St/BisGMA mixture modified with 5 wt% PMMA cured at 80 °C. Line connecting conversion points is drawn to guide the eye.

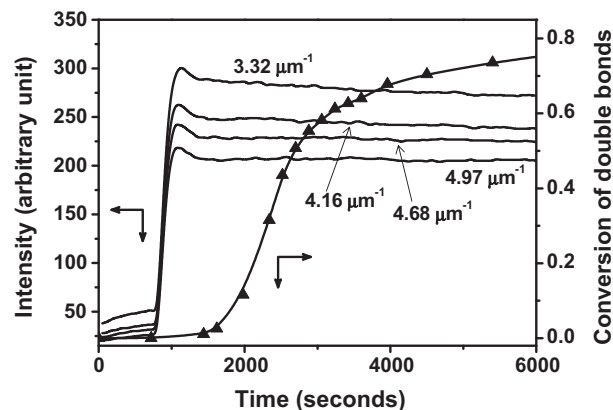


Fig. 3. Overall conversion of double bonds and light scattering intensity at different values of q vector plotted as a function of reaction time for the St/BisGMA mixture modified with 20 wt% PMMA cured at 80 °C. Line connecting conversion points is drawn to guide the eye.

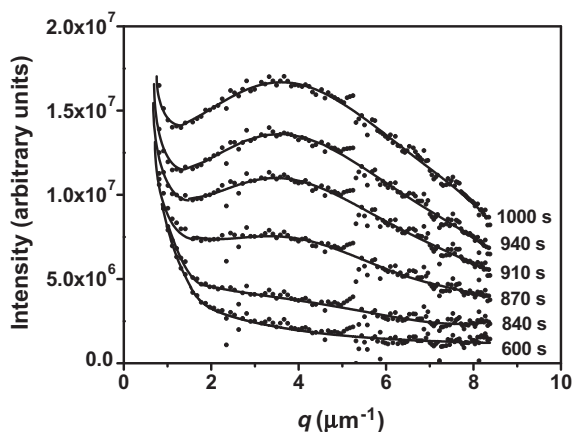


Fig. 4. Light scattering spectra at different reaction times for the sample modified with 20 wt% PMMA cured at 80 °C. Lines are drawn to guide the eye.

maximum located at a constant q value in systems undergoing a polymerization induced phase separation has been discussed in the literature and attributed to a spinodal decomposition mechanism frozen at early stages by viscosity or gelation [30,31]. According to this evidence, the evolution of the spinodal decomposition curves as a function of conversion was computed. The theoretical predictions and the comparison with the experimental results will be presented in the next section.

4.2. Evolution of the unstable region during polymerization

The proposed model in Section 2 allows to compute the evolution of the unstable region, limited by the spinodal curve, during the isothermal copolymerization of St and BisGMA in the presence or not of thermoplastic modifier. Table 1 summarizes the physical parameters used in the calculations, and Table 2 lists the values of the binary interaction parameters, which were evaluated in a previous work [27].

We first analyze the St/BisGMA system with no PMMA added. Shown in Fig. 5 is the calculated evolution of the unstable region (e.g. two-phase region) for this system polymerized at 80 °C. In the triangular diagram, St is placed in the upper vertex, BisGMA in the lower vertex at the left, and copolymer in the lower vertex at the right. The initial solution of St/BisGMA, denoted as F (45/55 wt%, equivalent to $\phi_{St} = 0.512$), is located on the left side of the triangle, and the compositional trajectory is represented by the thick line starting from F and ending, theoretically, in the vertex of pure copolymer.

Initially the mixture exists as a transparent homogeneous solution comprised by molecules of St and BisGMA.

Table 2

Constants a and b of the binary interaction parameters, χ_{ij} ($\chi = a + b/T$).

Binary pair	a	b (K)
St–BisGMA (χ_{01})	–0.330	325.1
St–PMMA (χ_{03})	0.085	131.3
BisGMA–PMMA (χ_{13})	–2.498	705.1

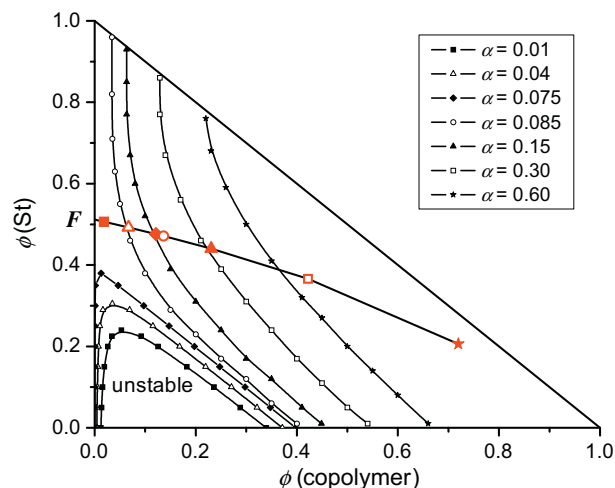


Fig. 5. Calculated evolution of the unstable region during copolymerization at 80 °C for the St/BisGMA sample without PMMA added. In the triangular diagram, St is placed in the upper vertex, BisGMA in the lower vertex at the left, and copolymer in the lower vertex at the right. Small points symbolize the spinodal curve at different conversion values whereas the corresponding larger points represent the composition of the system at the same conversion values. F denotes the initial solution of St/BisGMA (45/55 wt%, equivalent to $\phi_{St} = 0.512$) located on the left side of the triangle (St–BisGMA binary side).

When the double bond conversion is $\alpha = 0.01$, an unstable region extends from the base of the diagram (BisGMA–copolymer binary side) into the ternary field. This two-phase region is limited by the spinodal curve symbolized by small solid squares in Fig. 5. For the same conversion value ($\alpha = 0.01$), the composition of the system is represented by the larger solid square on the reaction trajectory. Since the composition point is above the unstable region, the system is homogeneous. As seen in Fig. 5, the two-phase region shifts upward and toward higher copolymer concentrations with increasing conversion, while the composition of the system moves along the trajectory as symbolized by the respective points. No phase separation is predicted in the pregel stage of the reaction ($\alpha < 0.08$) as the composition point falls always far above the respective spinodal curve.

For $\alpha = 0.085$, slightly above the gelation conversion, the unstable region extends across the ternary field including completely the binary BisGMA–St (left axis) of the diagram. This effect is produced by the elastic contribution to the mixing free energy (last term in Eq. (3)) due to the gel formation. Nevertheless, the composition of the system, represented by the unfilled circle in Fig. 5, falls outside of the two-phase region indicating that the system is still homogeneous. The same result was obtained for all the analyzed conversions in the postgel stage of the reaction ($\alpha > 0.08$) as shown in Fig. 5. Thus, the model predicts that the system (without PMMA added) never enters in the unstable region of the diagram and consequently remains in homogeneous state during the whole reaction. This result is in agreement with the experimental evidence previously presented.

We now analyze the St/BisGMA system modified with PMMA. During reaction, the system is comprised by four

components, St, BisGMA, copolymer, and PMMA. At a selected temperature, the graphical representation of such a system is a tetrahedron such as that illustrated in Fig. 6. Each corner represents the composition of one component of the system. The faces of this tetrahedron represent limiting ternary diagrams, similarly to the binary systems that are the limiting sides in a ternary diagram at a selected temperature. The spinodal boundary lines on the ternary diagrams extend into surfaces in the tetrahedron, and two-phase areas of the ternary systems become volumes in the quaternary system.

In the course of the copolymerization reaction, changes in the proportions of three of the four components (St, BisGMA, and copolymer) occur, while the concentration of PMMA remains constant. Thus, the compositional trajectory will be on a plane parallel to the base of the tetrahedron illustrated in Fig. 6. The intersection of this plane with the sides of the tetrahedron forms a triangle. As an example, we have shaded the triangle labeled $O'1'2'$ which corresponds to 20 wt% PMMA (Fig. 6). The arrow drawn from the side $O'1'$ to the vertex $2'$ represents the compositional trajectory for the selected example. It is instructive to note that the base of the tetrahedron shown in Fig. 6 corresponds to the triangular diagram presented in Fig. 5 for the system without PMMA added.

Then, to analyze the evolution of the unstable region in a quaternary system at a fixed PMMA concentration, we discuss the triangular diagram that results from considering the plane at constant PMMA concentration. In this triangle we represent the composition of the system and the spinodal boundary line for all the conversions analyzed. Note that the spinodal line is generated by the intersection of the spinodal surface in the tetrahedron with the triangular plane considered.

Fig. 7 shows the calculated evolution of the unstable region for the system modified with 5 wt% PMMA (equivalent to $\phi_{\text{PMMA}} = 0.064$) polymerized at 80 °C. Initially the mixture is in the one-phase homogeneous region of the diagram. When the double bond conversion is just $\alpha = 0.01$, the composition of the system enters in the

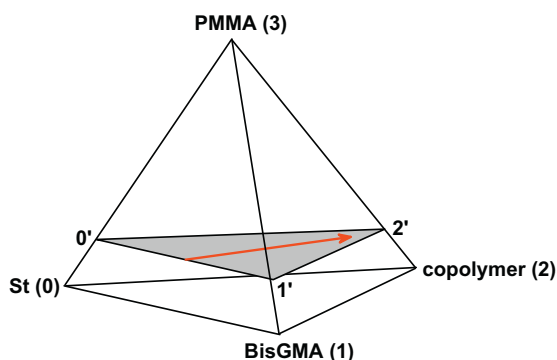


Fig. 6. Tetrahedral representation of a quaternary system composed by St, BisGMA, copolymer, and PMMA. The gray shaded plane (labeled $O'1'2'$) corresponds to 20 wt% PMMA ($\phi_{\text{PMMA}} = 0.178$). The red arrow drawn on this plane, from the side $O'1'$ to the vertex $2'$, represents the compositional trajectory during reaction for the sample with this amount of PMMA. (For interpretation of the references to color in this figure legend, the reader is referred to the web version of this article.)

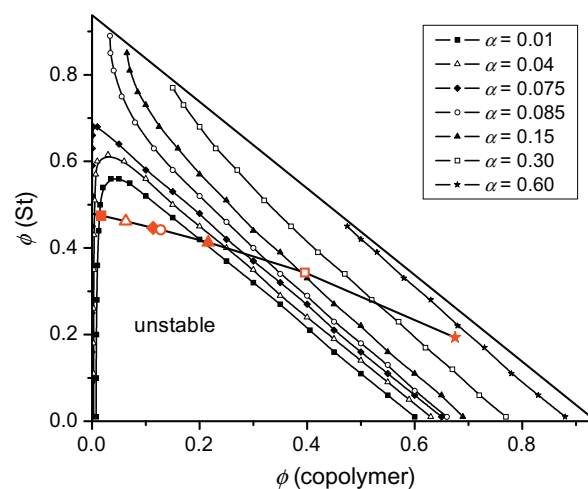


Fig. 7. Calculated evolution of the unstable region during copolymerization at 80 °C for the St/BisGMA sample with 5 wt% PMMA ($\phi_{\text{PMMA}} = 0.064$). Small points symbolize the spinodal curve at different conversion values whereas the corresponding larger points represent the composition of the system at the same conversion values. The model predictions corresponding to conversion values higher than the phase separation conversion were computed considering that each analyzed conversion is reached from a homogeneous state, as it is explained in the text. Note that in the represented plane the total mass of St, BisGMA, and copolymer represents a 95 wt% ($\phi = 0.936$) of the sample composition.

two-phase region as shown by the solid square point in Fig. 7. Consequently, the homogeneous solution becomes thermodynamically unstable and undergoes phase separation at very early stages of the polymerization reaction. This result is in very good agreement with the experimental evidence presented for the same system (Fig. 2), for which the phase separation begins at $\alpha = 0.02$.

Additional computations for conversion values higher than the phase separation conversion are included in this plot with the aim of showing the model predictions for the hypothetical case in which each analyzed conversion is reached from a homogeneous state. Note that this is a simplification, since once that the two phases have developed, the local composition and the resulting interactions are different and their evolution should proceed separately. However, the value of these predictions is that if the system is located in the unstable region of the phase diagram, it only can exist as a phase separated system. Actually, for all the analyzed conversions higher than 0.01 the system is located in the unstable region of the diagram as seen in Fig. 7. This result indicates that the sample remains phase separated during the rest of the reaction, prediction that is supported by the light scattering profiles shown in Fig. 2.

Simulations performed for the system with 20 wt% PMMA (equivalent to $\phi_{\text{PMMA}} = 0.178$) are presented in Fig. 8. For this system, the model also predicts that phase separation takes place at the beginning of the reaction. For a conversion value of $\alpha = 0.01$ the composition point falls almost on the spinodal curve symbolized by small solid square points in Fig. 8. As one can see, for any conversion value higher than 0.01 the system is located in the unstable region of the diagram and consequently it will be phase separated. This result is in good agreement with

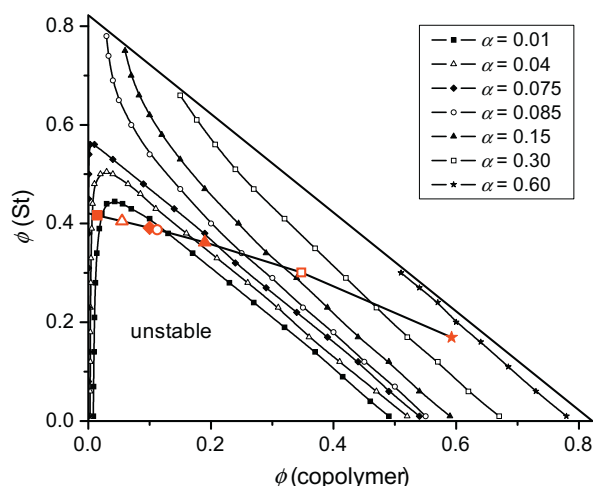


Fig. 8. Calculated evolution of the unstable region during copolymerization at 80 °C for the St/BisGMA sample with 20 wt% PMMA ($\phi_{\text{PMMA}} = 0.178$). Small points symbolize the spinodal curve at different conversion values whereas the corresponding larger points represent the composition of the system at the same conversion values. The model predictions corresponding to conversion values higher than the phase separation conversion were computed considering that each analyzed conversion is reached from a homogeneous state, as it is explained in the text. Note that in the represented plane the total mass of St, BisGMA, and copolymer represents only an 80 wt% ($\phi = 0.822$) of the sample composition.

the experimental behavior previously discussed (Fig. 3), evidencing the predictive capability of the proposed thermodynamic model.

5. Conclusions

Real-time static light scattering studies performed to monitor phase separation in the course of free-radical copolymerization of St and BisGMA, in the presence of PMMA as a modifier, showed the occurrence of a phase separation process at very early stages of the polymerization reaction ($\alpha = 0.02$, with 5 wt% of PMMA). This process occurred in the unstable region of the phase diagram by a spinodal decomposition mechanism as evidenced by the appearance of a scattering maximum located at a nonzero constant q value. The phase separation proceeds until the chain diffusion is strongly hindered by viscosity in the pre-gel stage of the reaction ($\alpha < 0.08$).

Co-continuous phase morphologies have been reported previously for these types of systems and have proved to be beneficial for a number of applications. In contrast to the experimental results, which may not be particularly surprising, an original and very interesting contribution was made in this work by modeling the evolution of the unstable region of the phase diagram as a function of conversion and by predicting phase separation in spinodal condition. The analysis was performed using an expression for the free energy of a reactive network-forming mixture based on the Flory–Rehner lattice model for swollen gels. For the selected formulations containing PMMA, the model predicts that phase separation takes place at almost the beginning of the reaction ($\alpha = 0.01$, at 5 wt% of PMMA), a result that is in good agreement with the experimental evi-

dence. On the other hand, for the sample with no PMMA added the model predicts that the system never enters in the unstable region of the diagram and consequently remains in homogeneous state during the whole reaction. This prediction is also in agreement with the presented experimental behavior, which is an indication of the accuracy of the proposed thermodynamic model.

Acknowledgements

The financial support of the National Research Council (CONICET), the National Agency for the Promotion of Science and Technology (ANPCyT), and the University of Mar del Plata, Argentina, is gratefully acknowledged.

Appendix A. Supplementary material

Considerations on the assumption that the total volume does not change upon reaction. Supplementary data associated with this article can be found, in the online version, at <http://dx.doi.org/10.1016/j.eurpolymj.2013.08.027>.

References

- [1] Echte A. In: Riew CK, editor. Rubber-toughened plastics. Washington (DC): American Chemical Society; 1989. p. 15–64.
- [2] Pascault JP, Williams RJJ. In: Paul DR, Bucknall CB, editors. Polymer blends, vol. 1. Formulation. New York; Wiley; 2000. p. 379–415.
- [3] Drzaic PS. Liquid cristal dispersions. Singapore: World Scientific; 1995.
- [4] Hoppe CE, Galante MJ, Oyanguren PA, Williams RJJ. *Macromolecules* 2004;37(14):5352–7.
- [5] Seo M, Hillmyer MA. *Science* 2012;336(6087):1422–5.
- [6] (a) Dubinsky S, Petukhova A, Gourevich I, Kumacheva E. *Macromol Rapid Commun* 2010;31(18):1635–40; (b) Dubinsky S, Petukhova A, Gourevich I, Kumacheva E. *Chem Commun* 2010;46(15):2578–80.
- [7] Pascault JP, Williams RJJ. In: Harrats C, Thomas S, Groeninckx G, editors. Micro- and nanostructured multiphase polymer blend systems. Boca Raton (FL): CRC Press – Taylor and Francis; 2006. p. 359–90.
- [8] Nakanishi K, Tanaka N. *Acc Chem Res* 2007;40(9):863–73.
- [9] Elbert DL. *Acta Biomater* 2011;7(1):31–56.
- [10] Zucchi IA, Galante MJ, Williams RJJ. *Polymer* 2005;46(8):2603–9.
- [11] Schroeder WF, Auad ML, Barcia Vico MA, Borrajo J, Aranguren MI. *Polymer* 2005;46(7):2306–19.
- [12] Soulé ER, Eliçabe GE, Borrajo J, Williams RJJ. *Ind Eng Chem Res* 2007;46(23):7535–42.
- [13] Rico M, López J, Montero B, Bellas R. *Eur Polym J* 2012;48(10):1660–73.
- [14] Schroeder WF, Borrajo J, Aranguren MI. In: Tsai LD, Hwang MR, editors. Thermoplastic and thermosetting polymers and composites. Hauppauge (New York): Nova Science Publishers, Inc.; 2011. p. 123–47 [chapter 4].
- [15] Seidl J, Malinský J, Dušek K, Heitz W. *Adv Polym Sci* 1967;5:113–213.
- [16] Williams RJJ, Borrajo J, Adabbo HE, Rojas AJ. In: Riew CK, Gillham JK, editors. Rubber-modified thermoset resins. Washington (DC): American Chemical Society; 1984. p. 195–213.
- [17] Williams RJJ, Rozenberg BA, Pascault JP. *Adv Polym Sci* 1997;128:95–156.
- [18] Rico M, López J, Montero B, Ramírez C, Bouza R. *Eur Polym J* 2011;47(8):1676–85.
- [19] Rico M, Lopez J, Díez FJ, Bellas R. *Eur Polym J* 2011;47(12):2432–41.
- [20] (a) Riccardi CC, Borrajo J, Meynie L, Fenouillot F, Pascault JP. *Polym Sci Part B Polym Phys* 2004;42(8):1351–60; (b) Riccardi CC, Borrajo J, Meynie L, Fenouillot F, Pascault JP. *Polym Sci Part B Polym Phys* 2004;42(8):1361–8.
- [21] Kamide K. Thermodynamic of polymer solutions: phase equilibria and critical phenomena. Amsterdam: Elsevier; 1990. Polymer Science, Library 9.

- [22] Soulé ER, Borrajo J, Williams RJJ. *Macromolecules* 2007;40(22):8082–6.
- [23] Wang X, Okada M, Han CC. *Macromolecules* 2007;40(12):4378–80.
- [24] Wang X, Okada M, Han CC. *Macromolecules* 2006;39(15):5127–32.
- [25] Boots HMJ, Kloosterboer JG, Serbutoviez C, Touwslager FJ. *Macromolecules* 1996;29(24):7683–9.
- [26] Serbutoviez C, Kloosterboer JG, Boots HMJ, Touwslager FJ. *Macromolecules* 1996;29(24):7690–8.
- [27] Schroeder WF, Yáñez MJ, Aranguren MI, Borrajo J. *J Appl Polym Sci* 2006;100(6):4539–49.
- [28] Inoue T. *Prog Polym Sci* 1995;20(1):119–53.
- [29] Cahn JW. *Chem Phys* 1965;42(1):93–9.
- [30] Alig I, Junker M, Schultz M, Frisch H. *Phys Rev B* 1996;53(17):11481–7.
- [31] Maugey J, Van Nuland T, Navard P. *Polymer* 2001;42(9):4353–66.
- [32] Flory PJ, Rehner JJ. *Chem Phys* 1943;11(11):521–6.
- [33] Dušek K, Dušková-Smrčková M. *Prog Polym Sci* 2000;25(9):1215–60.
- [34] Dušek K. Polymer networks: structural and mechanical properties. In: Chomppf AJ, editor. New York: Plenum; 1971, p. 245.
- [35] Boots HM, Kloosterboer JG, Serbutoviez C, Touwslager FJ. *Macromolecules* 1996;29(24):7683–9.
- [36] Schroeder WF, Aranguren MI, Borrajo JJ. *Appl Polym Sci* 2010;115(5):3081–91.
- [37] Merfeld GD, Paul DR. Polymer-Polymer Interactions Based on Mean-Field Approximations. In: Paul DR, Bucknall CB, editors. *Polymer blends, vol I: Formulation*. New York: Wiley; 2000 [55, *Advances in Chemistry Series* 233].
- [38] Okay O, Kurz M, Lutz K, Funke W. *Macromolecules* 1995;28(8):2728–37.
- [39] Auad ML, Aranguren MI, Borrajo J. *Polymer* 2000;41(9):3317–29.
- [40] Wagner HJ. *Phys Chem Ref Data* 1987;16(2):165–73.
- [41] Brill RP, Palmese GR. *J Appl Polym Sci* 2000;76(10):1572–82.
- [42] Schroeder WF, Borrajo J, Aranguren MIJ. *Appl Polym Sci* 2007;106(6):4007–17.
- [43] Boyard N, Vayer M, Sinturel C, Seifert S, Erre R. *Eur Polym J* 2005;41(6):1333–41.